Trans. JSASS Aerospace Tech. Japan
Vol. 12, No. ists29, pp. Pf_1-Pf_10, 2014

Original Paper

Laboratory Tests to Standardize Environment Test Conditions of Micro/Nano Satellite Units

By Amgalanbat BATSUREN, Kenta TOMIDA, Toru HATAMURA, Hirokazu MASUI and Mengu CHO

Kyushu Institute of Technology, Kitakyushu, Japan

(Received June 24th, 2013)

This paper presents the basic research for establishing the qualification test (QT) level a unit has to pass to be sold as a product for space usage. A laboratory test campaign was conducted to study how the mechanical stresses distribute within a satellite body so as to define the unit QT level. We carried out random vibration tests using two types 50cm/50kg class satellites and measured the distribution of acceleration inside the satellites. The research focuses on the provision of the physical basis of the test conditions to be defined in the new standard. We tried to identify the range of natural frequency and amplification of acceleration in various launching environment through statistical analysis of the test results. The detailed test procedure, analysis method and primary results are herein reported.

Key Words: Vibration Test, Acceleration, Natural Frequency, PSD, Dummy Satellite

Nomenclature

AT	:	acceptance test
DM	:	dummy mass
OBC	:	on board computer
PAF	:	payload adapter
PCU	:	power control unit
PSD	:	power spectrum density
Q	:	Q factor
QT	:	qualification test
RF	:	radio frequency unit

Subscripts

f	:	base frequency
f_0	:	resonant frequency
ζ	:	damping rate
n	:	sample number
p	:	probability of lager value
κ	:	frequency rate
s_y	:	standard deviation
t	:	transmittance
$\bar{y}$	:	average of sample

1. Introduction

As the uses of micro/nano satellites proliferate all over the world, there is an increasing need of improving their reliability. As the reliability expected for micro/nano satellites are different from that of the large/medium satellites, however, the test level, duration and precision may not be the same as those applied to the testing of large/medium satellites. Prior to now there have been environment test standards suitable only for large and medium sized satellites that demand very high reliability. For an example see Ref. 1). The existing standards are not suitable for micro/nano satellites that achieve low-cost and fast-delivery by using non-space qualified, Commercial–Off-The-Shelf (COTS) components extensively. The reliability expected for mirco/nano satellites is different from that of the large/medium satellites. There is a need of test standard to improve the reliability while keeping the nature of low-cost and fast-delivery. Currently there are confusion about testing approach among developers and customers about how the environment tests should be implemented for micro/nano satellites and their units.

In 2011, Nano-satellite Environment Test Standardization (NETS) project was initiated by a group made of Kyushu Institute of Technology, International Standard Innovation Technology Research Association, The Society of Japanese Aerospace Industries and AstreX to develop a environment test standard for micro/nano satellites.[1)] The word "micro/nano-satellite" in this paper is used for satellites that are mostly made of COTS units. Their weight and size is, **but not limited to,** typically less than 50kg and 50cm, respectively. NETS project is an international collaborative effort to establish an international standard for testing of micro/nano satellites. The project goal is to further the growth of worldwide micro/nano satellite activities and utilization by proposing affordable and reliable tests to the community.

There are various environment tests to be dealt with in NETS projects. In the present study, we deal with unit vibration test. At present, a large level of acceleration is applied to satellite units during the test, which has been derived by taking into account various safety margins. The bases of the margins are not always clear.

At the same time, there are many COTS-based units in the market, which are claimed to be good for micro/nano satellites.. Those products often however lack of test history under which they are qualified for the space use. Satellite developers are caught in the middle whether they choose an

expensive and long-delivery product weighing more emphasis on the reliability or choose the COTS-based product taking the risk of having a product that may not work in space. If the COTS-based product already passed a certain level of testing defined in a standard, the satellite developer may choose the COTS-based units with more confidence. Currently there is no such standard for micro/nano satellite units. One of the purposes of NETS project is to define the qualification test (QT) level the units have to pass to be sold as products for space use.

The NETS project aims at is meant to provide the minimum guarantee that a given unit sold as "a satellite unit" has a certain level of tolerance against space environment. Therefore, the unit QT in this standard does not include proper margin against the maximum predicted environment stress, which depends on each satellite. The satellite developers who procure the unit may carry out another QT using a dedicated test model. Note that as long as the unit uses COTS parts, there is a little guarantee that the test model is the same as the flight model. They may carry out PFT using a flight model or only AT taking the risk of little margin. The satellite developer shall provide the test levels and duration of the additional QT, AT or PFT.

The purpose of the present paper is to derive the unit QT level appropriate for the micro/nano satellite testing standard. We conducted random vibration tests using different acceleration ranges up to 9.0Grms with frequencies in the range of 20 to 2000Hz. Accelerometers inside satellites measured the distribution of mechanical stress. We investigated the resonant frequency, and amplification factor of each accelerometer position. The amplification factor is defined as the square root of the ratio of the measured PSD value at a given point by the base level as:

$$AF = \sqrt{\frac{PSD_m}{PSD_b}} \tag{1}$$

where AF is the Amplification factor, PSD_m is the measured PSD value, and the base PSD level is referred as PSD_b.

We calculated the resonance frequencies and the maximum amplification factor in the X, Y and Z vibration axes. We divided the vibration into three categories depending on the frequency ranges. We call the range between 20 and 300Hz whole satellite mode, because the vibration has strong signature associated with the resonance of the whole satellite body. The signature appears commonly among accelerometers at different locations. We call the ranges between 300 to 1000Hz and 1000 to 2000Hz, local vibration mode, because they are associated with resonance of individual structural components, such as an internal panel. The signature differs depending on the location of each accelerometer.

Ref. 2) dealt with whole satellite modes of six different micro satellites whose size and weight were mostly 50cm cube and 50kg. In the present paper, we deal with local vibration modes of two satellites. One of the two satellites, Hodoyoshi-3 was also included in the six satellites in Ref. 2). Combining the results with the ones of Ref. 2), we identify the resonant frequencies and the amplification factors between 20 and 2000Hz. Statistically estimating the interval of the resonant frequency range, we derive normal tolerance limits (NTL) on the amplification factor.

The paper is composed of four parts. The second part describes the experiment. The third part describes the results and their analysis and in the last the part overall experiment was summarized.

2. Experiment

We conducted the experiment by a shaker machine capable of 28kN rms random vibrations. We used experimental results of two satellites, Dummy satellite and Hodoyoshi-3 satellite as shown in Fig. 1 and Fig. 2 respectively to obtain the acceleration distribution inside the satellites. For the whole satellite modes, we used six satellites. The satellites we used are HODOYOSHI-2＆3, UNIFORM, RISESAT, RISING2, QSAT-EOS and TSUBAME.

The internal structure of the dummy satellite body is made of four panels with two third the width of the satellite body cross linked forming a "Yojo-han (four half tatami)" when viewed from the top, it can be seen as the popular layout of tatamis, Japanese traditional carpet. There is a square column made by the four panels at the center. The internal and external panels are made of Aluminum (alloy:5052). The dummy satellite is a copy of 50kg-50cm nano-satellite that was previously developed for remote sensing purpose as illustrated in Fig.1. The dummy satellite was made of basic satellite functions such as RF transmitter, PCU, battery and computer. See Ref. 3) for details. The other units are made by dummy mass with heater inside, the units. The satellite was fixed to the vibration machine using a mock-up of payload adaptor fitting (PAF) and a jig.

Hodoyoshi-3 is also an Earth remote sensing satellite of 50cm/50kg class. The test article used in the present research is its engineering model. Therefore, many of the internal units are still dummy mass. The basic structure of Hodoyoshi-3 satellite is a cube, to which two internal panels are fixed to mount different components. Two deployable solar panels attached to the satellite by a simple and reliable hold-release mechanism i.e. latch able hinge. In the present research, we use the test data obtained during its random vibration test.

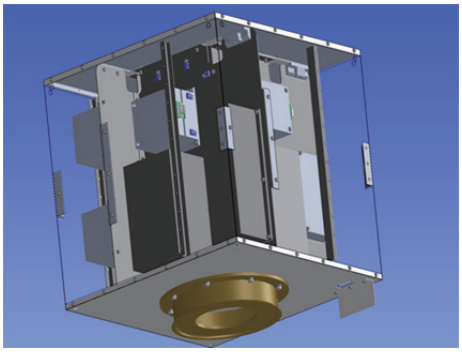

Fig. 1. Structure of the dummy satellite bus.

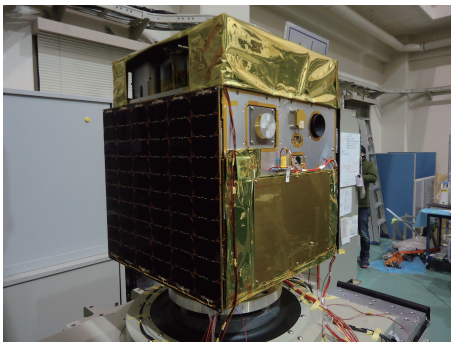

Fig. 2. Photo of Hodoyoshi-3 satellite.

For the dummy satellite, we measured at 46 points. Among the 46 points, 18 points were at dummy masses/units that were placed on internal panels. Fig. 3 shows some of the accelerometer positions. The accelerometers were attached to the internal panels of the satellite rather than the unit boxes. It is because the acceleration used for reference in the unit vibration test should be the ones of the base plate, i.e. the satellite internal panel.

For Hodoyoshi-3 satellite, we used the accelerometers data at 8 positions of inside panels. The measurement and analyzing philosophy of the Hodoyoshi-3 is similar to the dummy satellite.

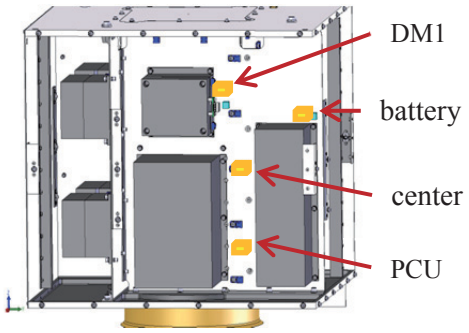

Fig. 3. Overview of the units and accelerometer positions on the dummy satellite (+X internal panel).

Each accelerometer was connected to a charge amplifier and the data was taken through a data acquisition box to a PC with USB cable. The maximum of 24 channels of the analog signal with the range of ±10V from the charge amplifier was taken simultaneously and converted to digital signal at 16 bit DAQ (5000 samples). Fast Fourier Transform (FFT) was applied by a standard desktop PC using Labview.

In the test, the vibration level was controlled by monitoring two monoaxial accelerometers (control accelerometer) attached rigidly on the jig aligned with the axis of applied vibration to check the input signal and taking the average of them (Fig. 4). Base accelerometers (ch23, ch24) for calculating amplification ratio were mounted besides the control accelerometers.

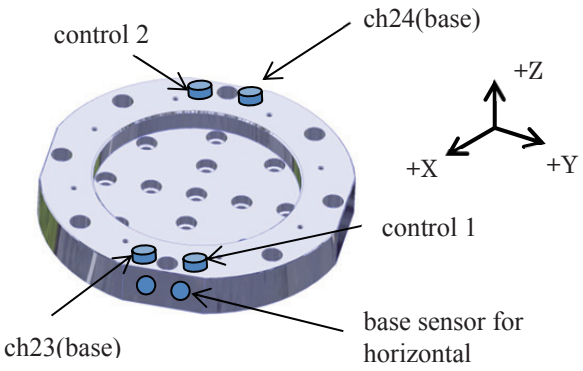

Fig. 4. Mounting position of base accelerometers on the jig.

Vibration tests were performed along the X, Y and Z satellite axes. Testing along the Z axis (parallel to the launcher axis) was performed mounting the satellite on the shaker using the jig. The same shaker and support, connected to the horizontal vibration table, were used for the X and Y axes vibration test (transverse vibration).

The base acceleration levels are shown in Figs. 5 and 6. For the Dummy satellite, the shape of input level comes from the Space and Missile Systems Center Standard (SMC). Using the same shape as shown in Fig. 5, the level was shifted so that we could test 5 levels, i.e. 0.3Grms, 1Grms, 3Grms, 6Grms and 9Grms. The test started from 0.3Grms toward 1.0Grms and 9.0Grms at the end. Each vibration was applied for 50 seconds. For Hodoyoshi-3, the base acceleration is based on the system QT level of 6.2 Grms specified by a launch provider as shown in Fig. 6. Each vibration test was also applied for 50 seconds.

In order to derive the vibration response at each point in the satellites, we used random vibration, instead of sinusoidal sweep due to two reasons. The first one is that the random vibration contains all the frequencies. Therefore, it is easy to derive the frequency response after carrying out the Fourier transform. The second is that the unit QT test to be carried out is random vibration test rather than sinusoidal sweep test.

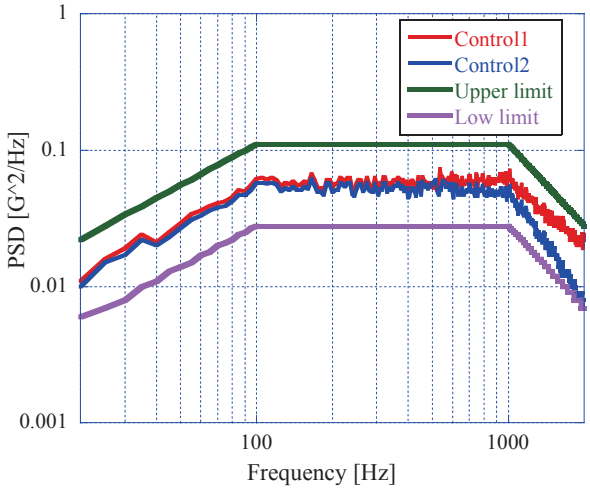

Fig. 5. Vibration profile of dummy satellite (9Grms).

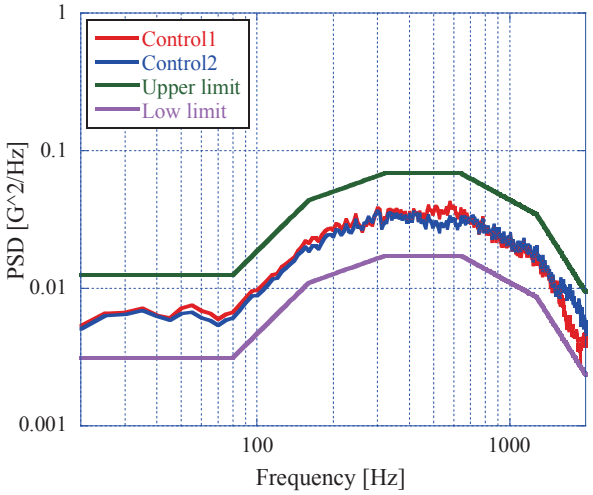

Fig. 6. Vibration profile of Hodoyoshi-3 (6.2Grms).

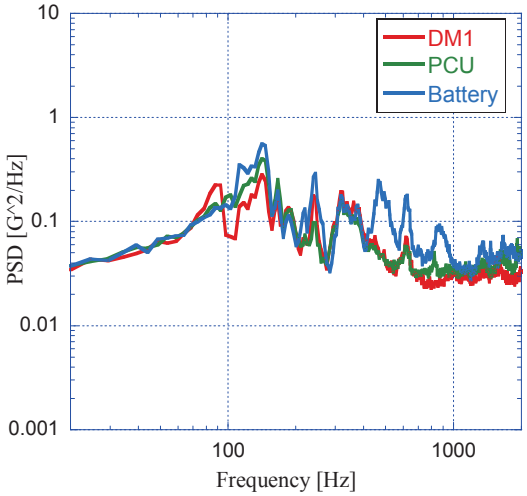

Fig. 8. PSD waveform (9Grms,axial direction vibration).

After each vibration, we checked the characteristic changes by performing a low level random, i.e. 0.3Grms to check if there are no changes for natural frequency etc.

3. Test Results and Data Analyzing

Figs. 7 and 8 show examples of the PSD waveform for the vibration in z-direction. The PSD values in the figures were measured from accelerometers to measure z axial acceleration attached to DM1, PCU and Battery that are placed at +x internal panel for the 0.3Grms and 9Grms input level. From the figures it can be seen that there is no significant difference in the resonant frequencies between the two vibration levels.

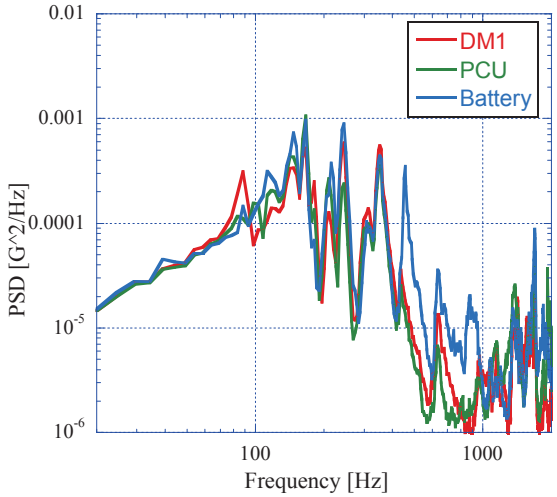

Fig. 7. PSD waveform (0.3Grms, z-axis sensor and z-axial direction vibration).

The amplification factor was calculated by using Eq.(1). Peak amplification factors were derived among the amplification factors corresponding to resonant frequency of each channel of measurement. Therefore, one value of the peak amplification factor exists for each PSD waveform unless we divide it into different frequency ranges as we do later.

Fig. 9 shows the maximum of the peak amplification factors for the various test level from 0.3Grms to 9Grms. Here, the maximum and minimum of peak amplification factors mean the maximum and minimum values among all the measurement points and the sensors of the same direction as excitation. In this test, the maximum value were 42, 32, 24, 21, 18 for 0.3Grms, 1Grms, 3Grms, 6Grms and 9Grms, respectively, as plotted in Fig. 9. The figure shows that peaks of amplification factor decreased with the increased base vibration level.

From Figs. 7 and 8, we can see that the peaks become smoother at higher G. It is because the vibration transmittance is not really a simple linear process. Non-linear effects smoothen the peak as the vibration force increases. Because our concern is whether units or a satellite can survive the harsh environment, we use the experimental results obtained from the high level acceleration to derive the unit test level. By using the result of the high level acceleration, the peak values in PSD are reasonably smoothed out and lead to a less severe test level.

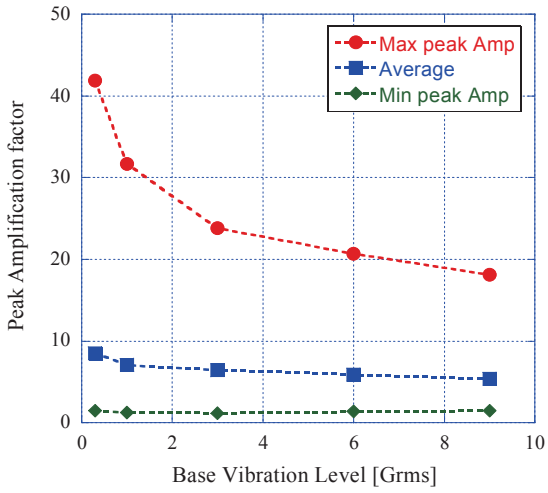

Fig. 9. Peak amplification factor comparison.

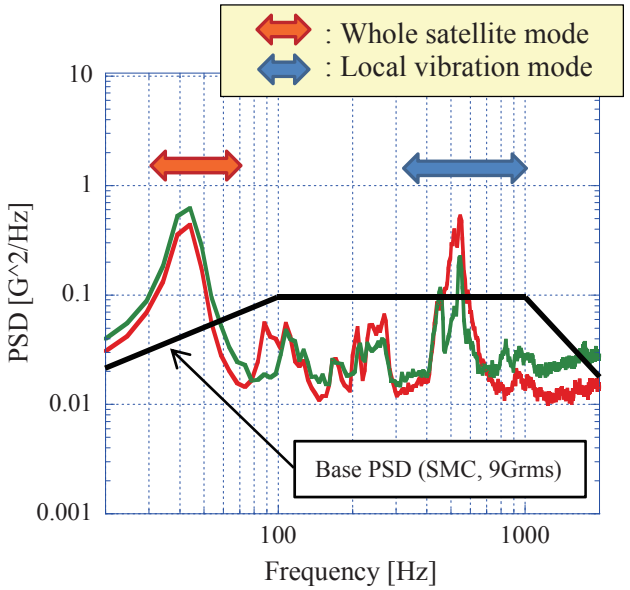

Fig. 10. Vibration response at internal panel (vibration is in the direction perpendicular to the axial direction).

Fig. 10 shows the example of PSD waveform measured at 9Grms when the base vibration is given in the direction parallel to the axis. We notice several features. Peaks at low frequencies are typically less than 300Hz. Those peaks originated from the resonance of entire satellite structures to the vibration. We call them "*Whole satellite mode*". In Ref. (2), we analyzed the whole satellite mode of various 50cm-class micro satellites. The resonances appeared between 29 and 70Hz for the vibration perpendicular to the thrust axis and 144 to 208Hz for the vibration parallel to the thrust axis. The results are updated later in this paper to derive the unit QT test level.

The peaks at frequencies higher than 300Hz (although the value 300Hz is rather arbitrary) are originated from the resonance of satellite internal structure. They depend on various factors, such as how the internal structure is arranged, direction/thickness/material of the internal panel, the sensor location, etc. We call those peaks "*Local vibration mode*". Internal units are exposed to those modes inside a satellite. To establish the standard test level, we needed to investigate the ranges of the whole satellite mode and local vibration mode in terms of the amplification factor at the resonant frequencies. We investigated the amplification factor and resonant frequency range for the local vibration mode (300-2000Hz) based on the statistical analysis similar to Ref. 2).

When we calculated the range of the amplification factor, the resolution of PSD became important. First we calculated and plotted PSD using 0.6Hz of frequency increment, Then, PSD was very high and sharp. If we had taken the statistics of the peak values, we would have seen extremely high level of acceleration, which is rather unrealistic. Unless the resonant frequencies of the satellite internal panel and the unit structure matches exactly, it is very unlikely that the unit will be accelerated at the high PSD value. The important thing is to give the energy contained within a certain bandwidth centered on the natural frequency.

Therefore, we changed *frequency increment* of the discrete Fourier transform from Δf=0.6Hz to Δf=4.8Hz to ensure smoother PSD. After changing the frequency increment to 4.8Hz, PSD became smoother than previous resolution. In order to check if we can use this frequency increment for our further analyzing, we compared RMS (Root Mean Square) of PSD for several frequency resolutions as listed in Table 1. We used the data of 6 different channels. Table 1 shows that there was no difference in RMS for different values of Δf. Therefore, we can give the energy properly to a unit even if we use the test level derived from the low resolution.

Table 1. RMS of PSD comparison in different frequency increment.

ch	Δf=0.6	Δf=1.2	Δf=2.4	Δf=4.8
1	9.64	9.64	9.64	9.64
2	16.60	16.60	16.60	16.60
3	9.18	9.18	9.19	9.19
4	11.30	11.30	11.30	11.30
5	23.30	23.30	23.30	23.30
6	10.00	10.00	10.00	10.00

In the local vibration mode, we collected data in the frequency range 300 to 2000Hz. We further divided the local vibration mode (300-2000Hz) into 2 groups: 300-1000Hz and 1000Hz-2000Hz. Because we noticed from the PSD waveform that in most cases there are several resonant frequencies from 300Hz to 2000Hz as seen in Fig. 10. Then we looked at all PSD in these two local vibration modes groups separately using 4.8Hz frequency resolution. We found peak PSD of resonant frequencies of all channels in each frequency group. In order to find resonant frequencies, we gathered PSD data of the accelerometers that measures the acceleration in the same direction as the vibration direction. In particular, we analyzed PSD data of X, Y, Z axis accelerometers' in the X, Y, Z vibration direction respectively. From the mechanical point of view, although the force perpendicular to the vibration direction is possible, this force is lower than that of the vibrating direction and is dependent on the satellite structure. Here X and Y vibration direction represents perpendicular to the axial direction and Z vibration direction represents the axial direction herein.

Tables 2 and 3 list the resonant frequency and the peak value of the amplification factor respectively observed at each measurement point inside the dummy satellite between 300 and 1000Hz. They are shown as examples to understand the statistical approach.

From these tables, we can deduce normal tolerance limits. Ref. 4 describes the way to calculate a conservative limit for the structural response spectra of a point to a point within a satellite structure in each frequency resolution band. Ref.4 says that there is considerable empirical evidence that the logarithm of the spectral values for any motion parameter describing the response from one point to another does have an approximately normal distribution; i.e., the spatial distribution of structural response spectra in a specific frequency resolution bandwidth approximately fits a lognormal distribution.

Table 2. Resonant frequency statistics (dummy satellite, 300-1000Hz).

	Resonant frequency[Hz]		
	Perpendicular to the axial(x)	Perpendicular to the axial(y)	Axial direction(z)
DM1	566.4	546.9	322.3
PCU	820.3	517.6	317.4
BATTERY	463.9	546.9	463.9
+X CENTER	566.4	546.9	336.9
DM6	546.9	927.7	302.7
OBC	561.5	302.7	341.8
RF	546.9	493.2	307.6
+Y CENTER	561.5	483.4	302.7
DM4	551.8	542.0	302.7
DM2	571.3	498.1	302.7
DM5	561.5	546.9	302.7
-X CENTER	532.2	498.1	302.7
DM3	571.3	498.1	302.7
DM9	537.1	996.1	302.7
DM7	566.4	961.9	302.7
DM10	537.1	493.2	356.5
-Y CENTER	566.4	498.1	302.7
DM8	566.4	659.2	302.7

Table 3. Peak value of amplification factor (dummy satellite, 300-1000Hz).

	Amplification factor		
	Perpendicular to the axial(x)	Perpendicular to the axial(y)	Axial direction(z)
DM1	1.35	2.83	1.69
PCU	2.50	5.97	1.54
BATTERY	4.31	1.85	2.18
+X CENTER	2.80	3.69	1.70
DM6	2.40	2.31	1.00
OBC	5.50	9.86	0.72
RF	3.07	8.48	1.41
+Y CENTER	3.98	3.66	1.21
DM4	1.80	0.99	1.16
DM2	2.50	4.35	1.22
DM5	2.38	1.05	1.52
-X CENTER	3.55	4.80	1.29
DM3	2.41	5.13	2.03
DM9	1.04	1.79	1.33
DM7	2.73	2.54	1.34
DM10	1.02	1.80	1.42
-Y CENTER	1.97	4.01	1.43
DM8	3.35	2.21	1.50

In order to compute a normal tolerance limit, we follow same methodology as the Ref. 4). Before this we also examined whether our tested data follow normal or lognormal distributions. In this reason, we plotted the values in Table 3 and their logarithm on probability plot sheet as shown in Figs. 11 and 12. When the data follows a straight line on the probability plot, the data follows a normal distribution. It is difficult to judge whether lognormal is better than the normal from these probability plot. We used χ^2 (Chi squared) goodness of fit statistics to check the normality of the test data distribution.

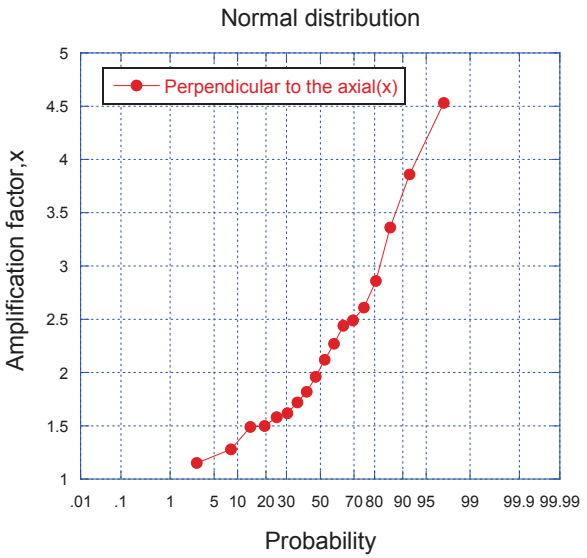

Fig. 11. Probability distribution (normal).

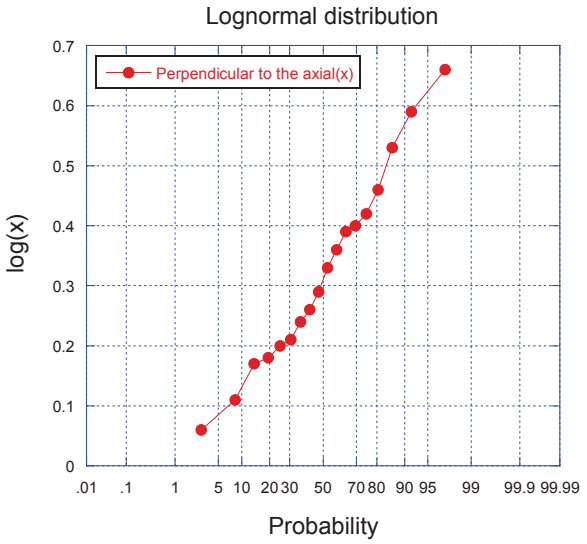

Fig. 12. Probability distribution (lognormal).

Normal and lognormal both looked good but lognormal was slightly better than normal. So after evaluating χ^2 (Chi squared) testing, we decided to choose the lognormal as the distribution of amplification factor. In order to evaluate, the *p*-value approach was used for both normal and lognormal distributions. The *p*-value is the probability of observing a sample statistic as extreme as the test statistic i.e. Chi-squared. On the other hand *p*-value is larger if the null hypothesis is true. In most cases, *p*-values of the lognormal distributions are more than normal distribution. In the example shown in Fig. 12, *p*- value was 0.91in lognormal while it was 0.62 in normal distribution as shown in Fig. 11. For the resonant frequency we chose a normal distribution.

A normal tolerance limit can be computed for the transformed predictions using Eq. (2). The Normal tolerance limit is defined as that value y that will exceed at least β

portion of all possible values of y with a confidence coefficient of γ, and is given by Eq. (3).

$$y = \log_{10} x \tag{2}$$

$$\mathrm{NTL}_y(n, \beta, \gamma) = \bar{y} \pm k_{n,\beta,\gamma}\ s_y \tag{3}$$

In Eq. (3), the term $k_{n,\beta,\gamma}$ is called the normal tolerance factor, and is a tabulated value which depends on the values of n, β and γ. We gathered the peak amplification factors and resonant frequencies related to each peak PSD value measured at 18 points located inside the dummy satellite. We used n=18 and $k_{n,\beta,\gamma}$ =1.67 for the dummy satellite while n=15 and $k_{n,\beta,\gamma}$ =1.68 for Hodoyoshi-3 data to calculate Normal tolerance limit using Eq. (2) and Eq. (3). Normal tolerance limit was chosen as 95/50 limit (β=0.95, γ=0.50) for both satellites data estimation.

Table 4. Resonant frequency range (dummy satellite, 300-1000Hz).

	Resonant frequency[Hz]		
	Perpendicular to the axial(x)	Perpendicular to the axial(y)	Axial direction (z)
Average	566.4	586.5	320.9
Standard deviation	281.0	760.4	161.0
Lower value	97.3	-683	51.1
Upper value	1035.7	1856.4	589.8

Table 5. Normal tolerance limit of amplification factor in logarithm of the dummy satellite in the range: 300-1000Hz (real values are shown in bracket).

	Amplification factor		
	Perpendicular to the axial(x)	Perpendicular to the axial(y)	Axial direction (z)
Average	0.39(2.4)	0.49(3.1)	0.14(1.4)
Standard deviation	0.20(1.6)	0.28(3.1)	0.11(1.3)
NTL (Min)	0.06(1.15)	0.02 (1.05)	0.04(1.1)
NTL (Max)	0.72(5.25)	0.96 (9.12)	0.32(2.09)

Table 6. Resonant frequency range (dummy satellite, 1000-2000Hz).

	Resonant frequency[Hz]		
	Perpendicular to the axial(x)	Perpendicular to the axial(y)	Axial direction
Average	1798.2	1798.2	1694.1
Standard deviation	864.7	1746.1	601.1
Lower value	354.1	-1117.8	690.3
Upper value	3242.2	4714.2	2697.9

Table 7. Normal tolerance limit of amplification factor in logarithm of the dummy satellite in the range: 1000-2000Hz (real values are shown in bracket).

	Amplification factor		
	Perpendicular to the axial(x)	Perpendicular to the axial(y)	Axial direction
Average	0.33(2.1)	0.32(2.1)	0.29(1.9)
Standard deviation	0.68(4.8)	0.70(5.0)	0.47(2.9)
NTL (Min)	-0.81 (0.15)	-0.85 (0.14)	-0.49 (0.32)
NTL (Max)	1.47(29.5)	1.49 (30.9)	1.07 (11.75)

Table 8. Resonant frequency range (Hodoyoshi-3, 300-1000Hz).

	Resonant frequency[Hz]		
	Perpendicular to the axial(x)	Perpendicular to the axial(y)	Axial direction
Average	576	464	501
Standard deviation	208	227	220
Lower value	206	60	109
Upper value	946	868	893

Table 9. Normal tolerance limit of amplification factor in logarithm of the Hodoyoshi-3 satellite in the range: 300-1000Hz (real values are shown in bracket).

	Amplification factor		
	Perpendicular to the axial(x)	Perpendicular to the axial(y)	Axial direction
Average	0.16(1.26)	-0.52(0.32)	-0.16(0.65)
Standard deviation	0.66(4.57)	0.67(4.68)	0.32(2.09)
NTL (Min)	-1.07(0.08)	-1.67(0.02)	-0.7(0.19)
NTL (Max)	1.2(15.85)	0.6(4.74)	0.3(2.01)

Table 10. Resonant frequency range (Hodoyoshi-3, 1000-2000Hz).

	Resonant frequency[Hz]		
	Perpendicular to the axial(x)	Perpendicular to the axial(y)	Axial direction
Average	1437	1689	1663
Standard deviation	345	380	326
Lower value	823	1013	1083
Upper value	2051	2365	2243

Table 11. Normal tolerance limit of amplification factor in logarithm of the Hodoyoshi-3 satellite in the range: 1000-2000Hz (real values are shown in bracket).

	Amplification factor		
	Perpendicular to the axial(x)	Perpendicular to the axial(y)	Axial direction(z)
Average	-0.28(0.52)	-0.79(0.16)	-0.34(0.45)
Standard deviation	0.44(2.75)	0.56(3.63)	0.37(2.34)
NTL (Min)	-1.02(0.09)	-1.73(0.02)	-0.96(0.11)
NTL (Max)	0.46(2.88)	0.15(1.41)	0.28(1.91)

The interval of the resonant frequency of the dummy satellite in the frequency range 300-1000Hz and 1000-2000Hz are listed in Table 4 and Table 6 respectively and the normal tolerance limit of the amplification factor of the dummy satellite are listed in Tables 5 and 7, respectively.

The data statistics of the Hodoyoshi-3 are shown in Tables 8-11. For Hodoyoshi-3 satellite, the number of measurement points of the internal panels was 15.

We now propose the unit QT test level with the estimated values. For simplicity, we first describe how we obtain the QT level using the result of the Dummy satellite only. Total of six (6) cases were studied for dummy satellite based on the local vibration mode using three (3) axes of the vibration direction namely; perpendicular to the axial direction(x), perpendicular to the axial direction(y) and axial direction (z) in particular for frequency ranges of 300-1000Hz and also for 1000-2000Hz.

In the selected frequency range we choose the amplification factor of 1.15 as the unit QT test level in the local vibration mode. 1.15 is the maximum number among the three values in the low tolerance limit as listed in Table 5. We choose this

maximum number at the low limit, because the test level we are trying to propose is to guarantee the minimum level of assurance. Unit manufacturers have no way of knowing in which direction their products will be mounted in the satellite. It could be on the plane perpendicular to the thrust axis or on the plane parallel to the thrust axis. At least it is possible that the product will undergo vibration amplified by a factor of 1.15 in one direction.

After determining the amplification factor for 300-1000Hz now we determine amplification factor and resonance frequency range for 1000-2000Hz interval. From the estimated values in Tables 6 and 7 the minimum tolerance limit of the amplification factors were 0.15, 0.14, 0.32 for directions perpendicular to the axial (x), (y) and axial (z) respectively. With the effect of damping due to structural fixations of the dummy satellite we have amplification to be less than 1. We can choose 0.32 as the amplification factor for the standard if we use the same logic for 300 to 1000Hz. Instead we select 1, no amplification, for the sake of simplicity. We simply take the amplification is uniform at unity between 1000 and 2000 Hz.

Now we modify the above mentioned number taking into account the result of Hodosyohi-3. Using the same logic, the maximum of low limit of the amplification factor is 0.19 between 300 and 1000 Hz and 0.11 between 1000 and 2000Hz. The value of 0.19 is smaller than 1.15 derived from the dummy satellite result. Therefore, we keep 1.15 in the 300-1000Hz range. The amplification factor stays 1 between 1000 and 2000Hz.

We selected 270Hz as the upper frequency range in the 20-300Hz frequency range and that will be explained later. We calculated the vibration transmittance apart from the resonance frequency ranges i.e. from 270Hz. Transmittance τ is described with damping rate ζ and frequency rate κ as shown in Eq. (4) and Fig. 13. We approximate the vibration by a single-degree-of-freedom vibration system. In addition, frequency rate κ is described with excited frequency of the base f and resonance frequency f_0 as shown in Eq. (5).[2)]

Damping rate ζ has the relation with Q factor (Amplification factor) as shown in Eq. (6). The quantity Q is a measure of the sharpness of resonance of a resonant vibratory system having a single degree of freedom. In a mechanical system, this quantity is equal to one-half the reciprocal of the damping ratio as shown in Eq. (6). It is commonly used only with reference to a lightly damped system and is then approximately equal to Transmittance or Transmissibility at resonance. Transmittance is the ratio of the response amplitude of a system in steady-state forced vibration to the excitation amplitude. In our case, transmittance is equal to the amplification factor.

Vibration transmittance at the outside of resonance frequency, i.e. from 270Hz, was calculated with resonance frequency f_0 and Q factor at boundary conditions. For calculating the gradient value from 270Hz to higher, we extrapolated the amplification factor and frequency until the amplification factor became 1.15 using Eq. (4). The amplification became 1.15 at 390Hz. We assumed ζ=0.1.

$$\tau = \sqrt{\frac{1+(2\zeta\kappa)^2}{(1-\kappa^2)^2+(2\zeta\kappa)^2}} \tag{4}$$

$$\kappa = \frac{f}{f_o} \tag{5}$$

$$Q \approx \frac{1}{2\zeta} \tag{6}$$

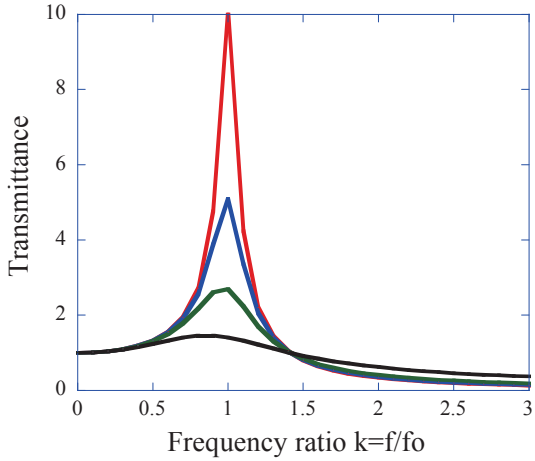

Fig. 13. Transmittance (τ) against frequency ratio (κ).

The amplification factor for whole satellite mode (20-300Hz) was calculated according to those procedures used in local vibration mode. Table 12 and Table 13 show the statistics of resonant frequency and amplification factor of whole satellite vibration modes of each satellite, respectively. The data were taken from the measurement point at either the top corner of the cubic satellites or the center of the panel facing the excited direction except the satellite-G. In the whole satellite mode, HODOYOSHI-2 & 3, UNIFORM, RISESAT, RISING2, QSAT-EOS, TSUBAME satellites' random vibration data were used, which are listed as Satellite A-G in Tables 12 and 13.

Table 12. Resonant frequency of each satellite (20-300Hz).

Satellite name	Resonant frequency[Hz]		
	Perpendicular to the axial direction 1	Perpendicular to the axial direction 2	Axial direction
Satellite-A	62	59	165
Satellite-B	56.3	43.8	165.6
Satellite-C	48.8	44.6	186
Satellite-D	44.6	40.9	144
Satellite-E	61	61	208
Satellite-F	32.3	29.3	144
Satellite-G	70	65	190

The data was taken from the result of QT random vibration test. As the satellite-G did not have accelerometers at neither the top corner nor the center of the panel, only the resonant frequencies are shown. These small-scale satellites (50cm・50kg) were developed in Japan. There are three whole satellite vibration modes against three axis of the satellite.

Table 13. Amplification factor of each satellite (20-300Hz).

Satellite name	Amplification factor		
	Perpendicular to the axial direction 1	Perpendicular to the axial direction 2	Axial direction
Satellite-A	8.2	10.4	8.0
Satellite-B	4.21	5.18	5.86
Satellite-C	6.52	5.75	7.56
Satellite-D	7.31	7.27	5.05
Satellite-E	5.73	6.92	3.39
Satellite-F	6.78	5.19	3.27
Satellite-G	-	-	-

With these results, we estimated interval of the resonant frequency and the normal tolerance limit of the amplification factor using same method as the one used for local vibration mode. The average of samples, low limit value, and high limit value have also been estimated as listed in Tables 14 and 15.

Table 14. Resonant frequency range (20-300Hz).

	Resonant frequency [Hz]		
	Perpendicular to the axial direction 1	Perpendicular to the axial direction 2	Axial direction
Average	54	49	172
Standard deviation	27	28	56
Lower value	6.7	0	74
Upper value	101.2	98	270

Table 15. Normal tolerance limit of amplification factor in logarithm in the range: 20-300Hz (real values are shown in bracket).

	Amplification factor		
	Perpendicular to the axial direction 1	Perpendicular to the axial direction 2	Axial direction
Average	0.80 (6.3)	0.82(6.6)	0.72(5.2)
Standard deviation	0.10 (1.2)	0.12(1.3)	0.17(1.5)
NTL (Min)	0.62 (4.2)	0.61 (4.1)	0.42 (2.6)
NTL (Max)	0.97 (9.3)	1.03 (10.7)	1.0 (10)

We deduce the vibration test level in the frequency range, 20-300Hz with these values using the same logic as before. In this case, we choose 4.2 as the unit QT level between 20Hz and 101Hz while the unit QT level was chosen as 2.6 in the 101Hz and 270Hz range. As explained before we extrapolated the amplification factor at 270Hz using Eq.(4), assuming ζ =0.1. Finally we merge the results of three frequency ranges and show the amplification factor of unit QT level between 20 and 2000Hz in Fig. 14.

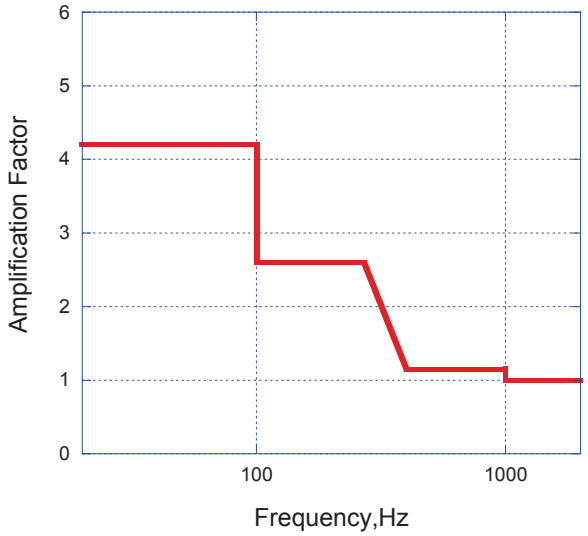

Fig. 14. The amplification factor and resonance frequency range for unit QT test level (20-2000Hz).

From now we give the base vibration level of the unit QT in terms of PSD. We multiply PSD of AT level of random vibration for various rockets in the frequency range of 20-2000Hz by the square of the amplification factor shown in Fig. 14. The result is shown as the unit QT level in Fig. 15. The unit QT level shown in red corresponds to the case where we used SMC AT level. It has an RMS value of 12.9Grms. The blue and green curves correspond to AT level of different rockets. The blue curve gives an RMS value of 11.8Grms, while the green curve gives 8.4Grms.

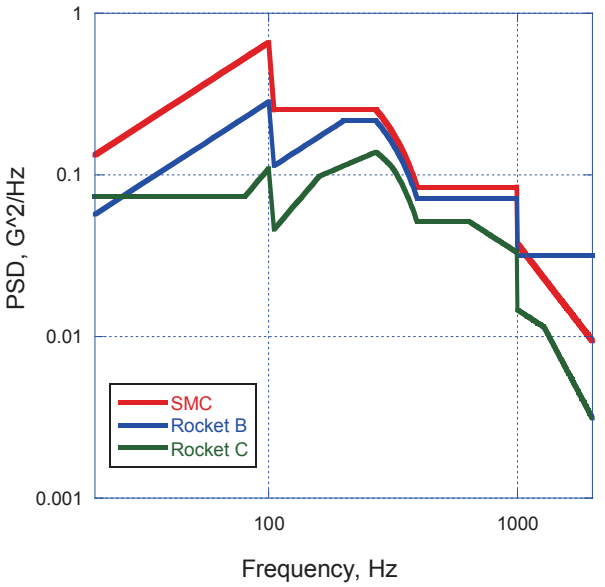

Fig. 15. Unit QT level (20-2000Hz).

It should be emphasized that the unit QT level shown in Fig. 15 is the only minimum level for each test article to obtain the minimum assurance that the product may survive the launch environment. Therefore, it does not contain any margin. If a satellite system integrator, the buyer of the product, wants to

set margin, they have to choose the test level by themselves based on the specifics of their satellites.

The QT level also do not account for any flight-to-flight variation. The level accounts for satellite-to-satellite variation among 6 or 7 satellites at frequencies less than 300Hz and 2 satellites at frequencies higher than 300Hz. We may need flight-to-flight variation if we are looking at the maximum limit. But we are trying to have the minimum limit. If we add the variation to the minimum number, the level will become very low. The level now is already low enough. We will accumulate more data of other satellites to improve the satellite-to-satellite variation or gather the data based on numerical analysis. We will include those to improve the statistics of this satellite.

4. Conclusion

NETS project for establishing environment test standard for micro/nano satellites started in 2011. In the present study, we dealt with basic research to define the qualification test (QT) level for COTS units in the framework of the NETS project.

We aimed to provide the minimum guarantee that a given unit sold as “a satellite unit” has a certain level of tolerance against space environment. The unit QT in the standard does not include proper margin against the maximum predicted environment stress, which depends on a satellite.

In order to determine unit QT level a series of random vibration test were conducted up to 2000Hz. Two test articles were used. They represent 50cm class satellites. We noticed two vibration modes, “whole satellite mode” and “local vibration mode”. We divided the measured data into three frequency ranges, 20 to 300Hz, 300 to 1000Hz and 1000 to 2000Hz. The first one corresponds to the whole satellite mode and the second and third ones correspond to the local vibration mode. We deduced the peak amplification factors and resonant frequencies within those three ranges. Based on statistical analysis refer to the Ref. 4), we defined the range of resonant frequencies and the normal tolerance limit of the peak amplification factors. The maximum value in the lower limits of the peak amplification among the three excited vibration directions was proposed as the unit QT level test.

In the present paper, we used data of six satellites to deduce the whole satellite mode. But we used data of only 2 satellites to deduce the local vibration mode. In order to cover wide range of structural styles expected in micro/nano satellites, we will carry out structural analysis using a finite element analysis (FEA) software. In the analysis, we will calculate the acceleration inside various types of satellites. The results will be used to update the unit QT level proposed in the present paper.

Acknowledgments

The authors are grateful for the following satellite projects for providing the satellites vibration test data; Hodoyoshi project, UNIFORM project, RISESAT project, RISING2 project, QSAT-EOS project and TSUBAME project. The authors thank for the encouragement and support provided by Prof. Kuniaki Shiraki, Kyushu Institute of Technology and the members of NETS committee for their valuable comments.

HODOYOSHI 3 and 4 were developed under “New Paradigm of Space Development and Utilization by Nano-satellite" granted by the Japan Society for the Promotion of Science (JSPS) through the “Funding Program for World-Leading Innovative R&D on Science and Technology (FIRST Program),” initiated by the Council for Science and Technology Policy (CSTP).

References

1) Cho, M., Date, K., Horii, S. and Obata, S.: Introduction of Nanosatellite Environment Test Standardization (NETS) Project, Background and Objectives, Joint-Conference on Space Technology and Science, 2011, JSASS-2011-4424.
2) Tomida, K., Batsuren, A., Hatamura, T., Masui, H. and Cho, M.: Basic Research on Vibration Test Level for Nanosatellite Components, 29th International Symposium on Space Technology and Science, 2013, 2013-f-26.
3) Onishi, S., Aso, S., Ohta, H., Murozono, M. and Yasaka, T.: Thermal and Structural Design of QSAT-EOS, Proceedings of 28th International Symposium on Space Technology and Science, 2011, 2011-f-29.
4) Dynamic Environmental Criteria, NASA-HDBK-7005, 2001.